*2023 International Research Conference of Sri Lanka Technology Campus*
*Colombo, Sri Lanka. 14th-15th December 2023*

# Modal Analysis of Rectangular-Shaped Concrete Liquid Storage Tanks with Baffles

H.A.R.S. Fonseka
*National Water Supply & Drainage Board*
*Colombo, Sri Lanka*
sulaknaf@yahoo.com

K.A.S. Susantha
*Department of Engineering Mathematics*
*University of Peradeniya*
Peradeniya, Sri Lanka
samans@pdn.ac.lk

***Abstract*—This study focuses on the modal analysis of rectangular-shaped concrete fluid storage tanks with internal baffles. Liquid sloshing, occurring during earthquakes, presents engineering problems due to the interaction between the liquid and the tank. Modal analysis is employed to determine the fundamental frequency characteristics, validating the results with previous work. It is figured that baffles can be employed to distance the excitation frequency from both the fundamental resonant frequency and any other resonant frequency. Ansys software is used to examine the effect of internal objects on mode shapes and natural frequencies in a concrete rectangular fluid tank system.**

***Keywords—Modal analysis, liquid storage tanks, baffles***

## I. Introduction

Modal analysis is a parameter which is fundamental to any system subjected to dynamic loading. Sloshing characteristics such as mode shapes and natural frequencies depend on the material characteristics and geometry of the liquid system, liquid-filled depths, and the restraint types at the tank boundaries. The presence of internal submerged components in the tank alters the total characteristics of the free and forced vibration systems.

Several studies related to fluid sloshing have been carried out analytically, numerically, and experimentally, but a limited number of studies reported on the modal analysis considering the presence of internal objects. Free vibration characteristics are attained using the non-linear formulation. In the baffled scenario, the size and location of the submerged baffle are varied.

## II. Mathematical Background of Model Analysis

### A. Modal Analysis-Acoustics

Finite Element Analysis (FEA) can be employed to compute the response of a complex structure subjected to forcing functions, which may involve an acoustic source or a distribution of mechanical forces. FEA of acoustic systems entails the discretization of the acoustic volume into elements and nodes. A confined acoustic space might be surrounded by rigid walls, a flexible structure, or walls that deliver acoustic damping.

The finite element method (FEM) considers the mutual interaction between a structure and a fluid whether it's air or water. In challenges involving acoustic fluid-structure interaction, we must account for the equations governing structural dynamics. This includes incorporating the mathematical representation of the system's acoustics as described by the Navier-Stokes equations of fluid momentum and the flow continuity equation. The discretized equation for structural dynamics can be formulated using structural finite elements. The fluid momentum and continuity equations undergo simplification to derive the acoustic wave equation, including assumptions such as fluid compressibility and inviscidity as in [1].

The acoustic wave equation serves as a tool for describing the acoustic response of the fluid. Appropriate acoustic finite elements can be developed by discretizing the lossless wave equation through the Galerkin method. There are two formulations of finite elements that are used to analyze acoustic problems considering either pressure or displacement as the unknown. The most common and used FE in this modal analysis is the pressure-formulated element as in [1].

### B. Pressure Formulated Acoustic Elements

The acoustic pressure $P$ in a FE can be shown as;

$$P = \sum_{i=1}^{m} NiPi \quad (1)$$

Where $N_i$ is a set of linear shape functions, $P_i$ are acoustic nodal pressures at node $i$, and $m$ is the number of nodes forming the element. For pressure-formulated acoustic elements, the FE equation for the fluid is,

$$[M_f]\{\ddot{P}\} + [K_f]\{P\} = \{F_f\} \quad (2)$$

Where $[K_f]$ is the equivalent fluid stiffness matrix, $[M_f]$ is the equivalent fluid mass matrix, $F_f$ is a vector of applied fluid loads, P is a vector of unknown nodal acoustic pressures, and $\ddot{P}$ is a vector of the second derivative of acoustic pressure with respect to time. FLUID 220 is one of the available acoustic elements in ANSYS [2], and used in the modal acoustic analysis as a fluid domain [1].

### C. Fluid-Structure Interactions (F-S-I)

Standard pressure-formulated acoustic elements can be connected to structural elements so that the two become coupled, hence the acoustic pressure acts on a structure which causes it to vibrate, and also is the converse where a structure which vibrates causes sound to be produced in an acoustic fluid.

The Equation for the coupled fluid-structure interaction is,

$$[M_s]\{\ddot{U}\} + [K_s]\{U\} = \{F_s\} \quad (3)$$

Where $[K_s]$ is the structural stiffness matrix, [M] is the structural mass matrix, $\{F_s\}$ is a vector of applied structural loads, {U} is a vector of unknown nodal displacements and $\{\ddot{U}\}$ is a vector of the second derivative of displacements

with respect to time, equivalent to the acceleration of the nodes. The F-S-I occurs at the interface between the structure and the acoustic elements, where the acoustic pressure exerts a force on the structure and the motion of the structure produces a pressure. To incorporate the coupling between the structure and the acoustic fluid, additional terms are added to the equations of motion for the structure and fluid (of density, $\rho_o$), respectively, as given below [1].

$$[M_s]\{\ddot{U}\} + [K_s]\{U\} = \{F_s\} + [R]\{P\} \quad (4)$$

$$[M_f]\{\ddot{P}\} + [K_f]\{P\} = \{F_f\} - \rho_o\,[R]^T\{\ddot{U}\} \quad (5)$$

Here, [R] is the coupling matrix that accounts for the effective surface area associated with each node on the fluid-structure interface. The above equations can be formed as matrices as given in Eq. (6) [1];

$$\begin{bmatrix} Ms & 0 \\ \rho_o R^T & Mf \end{bmatrix}\begin{Bmatrix} \ddot{U} \\ \ddot{P} \end{Bmatrix} + \begin{bmatrix} Cs & 0 \\ 0 & Cf \end{bmatrix}\begin{Bmatrix} \dot{U} \\ \dot{P} \end{Bmatrix} + \begin{bmatrix} Ks & -R \\ 0 & Kf \end{bmatrix}\begin{Bmatrix} U \\ P \end{Bmatrix} = \begin{Bmatrix} Fs \\ Ff \end{Bmatrix} \quad (6)$$

Where $[C_s]$ and $[C_f]$ are structural and acoustic damping matrices.

The fluid-structure interaction method described above accounts for two-way coupling between structures and fluids. When using this coupling in FEA, it is required to construct the model to represent the interface between the fluid and the structure. The elements for the structural partition contain displacement Degree of Freedoms (DOFs). At the interface between the acoustic fluid and the structure, there is a single layer of acoustic elements that have pressure and displacement DOFs. It is this thin layer of elements that enables the mutual coupling between the vibration of the structure and the pressure response in the liquid. While it is feasible to employ acoustic elements with both pressure and displacement DOFs throughout the entire acoustic field, this is unnecessary and leads to prolonged solution times. A more efficient strategy involves utilizing elements with both types of DOFs only at the fluid-structure interfaces and employing acoustic elements with solely a pressure DOF for the remaining acoustic field. When utilizing ANSYS software [2], it becomes imperative to explicitly specify the contact surfaces between the structure and the fluid by using the Fluid-Structure-Interface (FSI).

## III. Model Analysis of Concrete Rectangular-Shaped Tanks

### A. Finite Element Modelling

In Ansys workbench, the ACT extension modal acoustics is used. Frictionless contact between fluid and tank, free surface, fixed base, fluid-acoustic and tank-physics configuration, gravity, and fluid-solid interface are considered. An acoustic analysis can compute either the propagation properties of pure acoustic waves within a specified environment or the coupled acoustic F-S-I using either the Helmholtz or convective wave equation as in [1]. Four types of elements used; SOLID185 – for 3-D modelling of solid structures, FLUID220 – for 3-D modelling of fluid medium, TARGE170 – denotes various 3-D target surfaces for the associated contact elements, CONTA174 – denotes contact and sliding between target surfaces and a deformable surface defined by this element as in [1].

### B. Modal Analysis Validation

The hydrodynamic pressure resulting from dynamic loading is divided into impulsive and convective components. The impulsive pressure arises from the liquid segment accelerating with the tank, while the convective pressure is generated by the oscillation of the liquid portion within the tank. The present model, slightly modified, has been embraced in many codes and standards. To validate the FE model, the fundamental periods of both the impulsive and convective modes for the rectangular tank were determined and subsequently compared with the analytical solution proposed by Housner. [3] along with selected design codes such as EC8, ACI 350.3, and ECP 201.

#### 1) Description of the model

A fixed base shallow rectangular concrete tank with dimensions of 30.0 m length (Lz), 15.0 m width (Lx) and, 6.0 m wall height (Hw) has been used. The wall thickness of the tank (tw) is 0.60 m and the height of the liquid inside the tank ($H_L$) is 5.50 m. This tank was previously used by several researchers such as Kianoush and Chen [4], Chen and Kianoush [5], Kim et al. [6] and, Yazdanian and Ghasemi [7]. A schematic configuration of the tank is shown in Fig. 1. The material properties of the concrete and liquid are listed in Table 1.

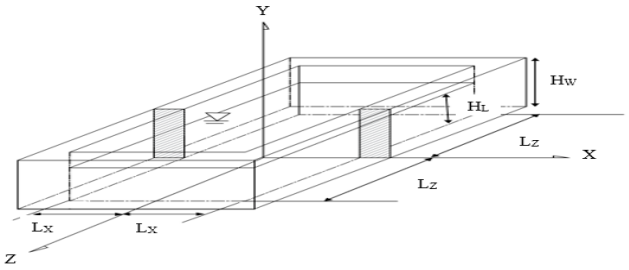


Fig. 1. An illustrative diagram representing the tank under consideration.

TABLE 1. MATERIAL PROPERTIES OF LIQUID AND TANK

| Concrete | | | Liquid | |
|---|---|---|---|---|
| ***Young's modulus ($E_c$)*** | ***Density $\rho_c$*** | ***Poisson's ratio $\upsilon$*** | ***Density $\rho_w$*** | ***Bulk modulus*** |
| $2.644\times10^{10}$ Pa | 2300 kg/m$^3$ | 0.17 | 1000kg/m$^3$ | $2.1\times10^9$ Pa |

#### 2) Comparison of FE results

The fundamental periods of both the impulsive and convective modes for the shallow rectangular tank were determined and compared with the analytical solution proposed by Housner [3], in Safaa et al. [8]. Hence, the modal analysis was employed and the resulting natural frequencies for the impulsive (Ti) and the convective (Tc) modes have been documented in Table 2 and compared with the analytical results. Additionally, the fundamental mode shapes of the shallow rectangular tank are shown in Fig. 2.

TABLE 2. COMPARISON AMONG FE AND ANALYTICAL RESULTS

| Fundamental Period(s) | Ansys Simulation Results | Analytical (Housner) | %Difference |
|---|---|---|---|
| Impulsive (Ti) | 0.138 sec (7.22 Hz) | 0.15 | -8.6% |
| Convective (Tc) | 8.60 sec (0.116Hz) | 8.56 | +0.4% |

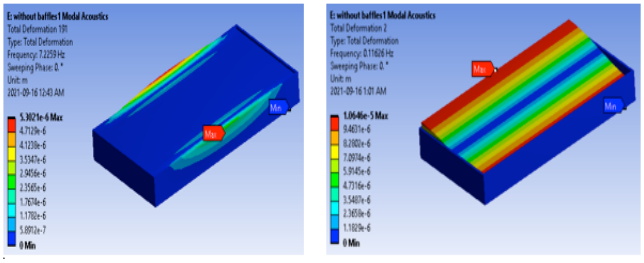

(a) Impulsive mode shape Ti = 0.138 s (7.22Hz)

(b) Convective mode shape Tc = 8.6 s (0.116Hz)

Fig. 2. Fundamental mode shapes

TABLE 3. EXPRESSIONS FOR CONVECTIVE AND IMPULSIVE TIME PERIODS GIVEN IN DIFFERENT CODES

| Reference | Expression | |
|---|---|---|
| | ***Impulsive*** | ***Convective*** |
| Eurocode 8 part 4: equations - A.46 & A.47 | $T_i=2\pi\{d_f / g\}^{1/2}$ | $T_c = 2\pi\{L/g\}^{1/2} / \{(\pi/2)\tanh((\pi/2)(H/L))\}^{1/2}$ |
| ACI 350.3 | $T_i =2\pi\{(W_i + W_w)/g_k\}^{1/2}$ | $T_c = 2\pi\{L\}^{1/2} / \{(3.16g)\tanh(3.16(H/L))\}^{1/2}$ |
| ASCE 7 | No expressions given | $T_c = 2\pi\{L\}^{1/2} / \{(3.68g)\tanh(3.68(H/L))\}^{1/2}$ |
| ECP - 201 | $T_i = 2\pi\{d_f / g\}^{1/2}$ | $T_c = 2\pi\{L/g\}^{1/2} / \{(3.16)\tanh((3.16)(H/L))\}^{1/2}$ |

TABLE 4. COMPARISON BETWEEN ANSYS RESULTS AND DIFFERENT SEISMIC DESIGN CODES FOR THE CONVECTIVE MODE

| Design code | Ansys Simulation | EC 8 – part 4 | ACI 350.3 | ECP-201 |
|---|---|---|---|---|
| $T_c$ (s) | 8.6 | 8.59 | 8.55 | 8.55 |
| %Difference | - | -0.1 % | -0.5 % | -0.5% |

## C. *Parametric Study*

The natural frequencies and mode shapes are figured in two types of tanks, namely, shallow and tall tanks. The dimensions of these tanks are derived from previous works by Kim et al. [6], Kianoush and Chen [4], Chen and Kianoush [5] and, Yazdanian and Ghasemi [7].

In the study by Kim et al [6], the effect of the length-to-height ratio, $2Lz/H_W$ was studied among various geometric factors, while other dimensions and material properties remained constant. The study considered a range of the ratio $1<2Lz/H_W<20$. Fundamental frequencies for different ratios of $2Lz/H_W$ were calculated by 3-dimensional models and compared with those from 2-dimensional models. It was perceived that as the aspect ratio increased, the fundamental frequency converged with that of the 2-dimensional model, irrespective of 3-dimensional restraint conditions. At a ratio of $2Lz/H_W = 10$, the fundamental frequency is closely aligned with that of the 2-dimensional model. Beyond $2Lz/H_W>10$, the change of fundamental frequency became insensitive to the ratio. This indicates that response characteristics do not significantly change in the range of 2Lz/Hw, as corroborated study's results. Peak relative displacement and peak total acceleration at the top of the middle cross-section of the side wall were calculated and presented for varying length-to-height ratios ($2Lz/H_W$).

Even though the outcomes in the study by Kim et al [6] study were derived from time-domain analysis without damping, they clearly indicate a consistent trend. When the ratio $2Lz/H_W$ is higher than 10, the responses tend to remain relatively constant. Conversely, when the ratio is smaller than 10, the responses appear to be significantly affected by the length-to-height ratio. It is important to note that the response itself was not identical to that of the 2-dimensional model, as outlined in the study, where hydrodynamic pressure distributions over the flexible wall surface were plotted for the length-to-height ratio 20. Therefore, the dimensions of two tanks labeled "shallow" and "tall", which demonstrate the outcomes of the influence of $2Lz/H_W$, were considered in this study.

- Shallow tank –

  Lx = 15m, Lz = 30 m (L=60m), Hw = 6m, $H_L$ = d = 5.5m, $t_w$ = 0.6m

- Tall tank –

  Lx = 9.8m, Lz = 28 m (L=56m), Hw = 12.3m, $H_L$ = d = 11.2m, $t_w$ = 1.2m

The investigation involves exploring the impact of submerged baffles on the free vibration characteristics of sloshing by varying their sizes and positions. In Ansys simulation, impulsive and convective fundamentals can be figured without hesitation as the difference of model shapes are obvious. The first few frequencies are considered for each impulsive and convective mode.

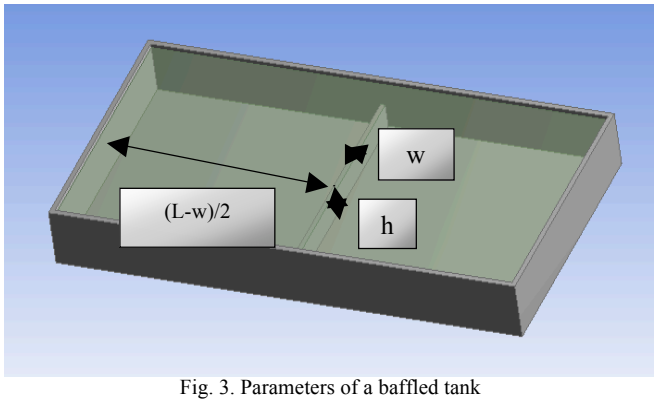


Fig. 3. Parameters of a baffled tank

The effects of centrally placed and off-centered baffle/baffles on the sloshing frequencies and mode shapes are considered. A parametric study is conducted considering the following as variables;

*1)*. Width of baffle to length (w/L)
*2)*. Baffle height to water depth ratio (h/d)
*3)*. Location of the baffle, i.e. 0.5L and 0.25L
*4)*. Number of baffles

TABLE 5. PARAMETERS OF THE RECTANGULAR TANKS

| | | | |
|---|---|---|---|
| Shallow Tank d / L = 5.5 / 60 = 0.09 | h / d = 1.375 / 5.5 = 0.25 | h / d = 2.75 / 5.5 = 0.5 | h / d = 4.95 / 5.5 = 0.9 |
| | w / L = 0.6 / 60 = 0.01 | w / L = 1.8 / 60 = 0.03 | h / d = 3.6 / 60 = 0.06 |
| Tall Tank d / L = 11.2 / 56 = 0.2 | h / d = 2.8 / 11.2 = 0.25 | h / d = 5.6 / 11.2 = 0.5 | h / d = 10.08 / 11.2 = 0.9 |
| | w / L = 0.56 / 56 = 0.01 | w / L = 1.68 / 56 = 0.03 | w / L = 3.36 / 56 = 0.06 |

### *1) The Effect of Baffle Width and Tank Length (w/L)*

TABLE 6. FREQUENCIES (HZ) ON CENTRALLY PLACED BAFFLE WITH VARYING H/D AND W/L – SHALLOW TANK

| d/L | h/d | j = mode number | w/L= 0 (No baffle) | w/L= 0.01 | w/L= 0.03 | w/L= 0.06 |
|---|---|---|---|---|---|---|
| 0.09 | 0.25 | 1 | 0.060 | 0.059 | 0.059 | 0.058 |
| | | 2 | 0.116 | 0.116 | 0.115 | 0.115 |
| | | 3 | 0.116 | 0.116 | 0.116 | 0.116 |
| | | 4 | 0.128 | 0.128 | 0.128 | 0.127 |
| | | 5 | 0.157 | 0.157 | 0.156 | 0.156 |
| | 0.5 | 1 | 0.060 | 0.057 | 0.056 | 0.055 |
| | | 2 | 0.116 | 0.116 | 0.115 | 0.114 |
| | | 3 | 0.116 | 0.116 | 0.116 | 0.115 |
| | | 4 | 0.128 | 0.127 | 0.127 | 0.126 |
| | | 5 | 0.157 | 0.156 | 0.156 | 0.155 |
| | 0.9 | 1 | 0.060 | 0.047 | 0.042 | 0.037 |
| | | 2 | 0.116 | 0.115 | 0.114 | 0.111 |
| | | 3 | 0.116 | 0.116 | 0.115 | 0.114 |
| | | 4 | 0.128 | 0.124 | 0.123 | 0.121 |
| | | 5 | 0.157 | 0.144 | 0.138 | 0.135 |

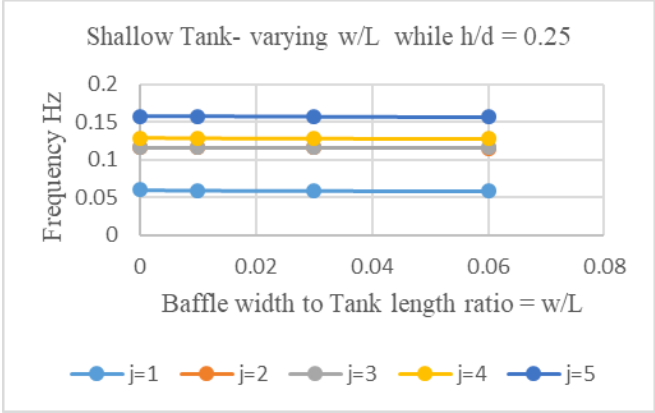


Fig. 4. Shallow Tank- Natural frequency variation of baffle width to tank length (w/L) while baffle height to fluid depth (h/d) =0.25

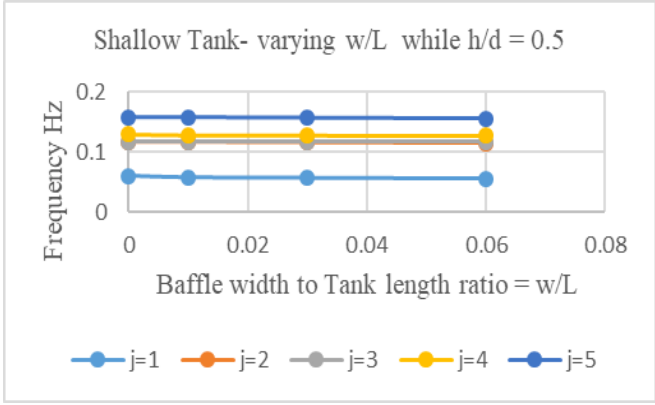


Fig. 5. Shallow Tank- Natural frequency variation of baffle width to tank length (w/L) while baffle height to fluid depth (h/d) =0.5

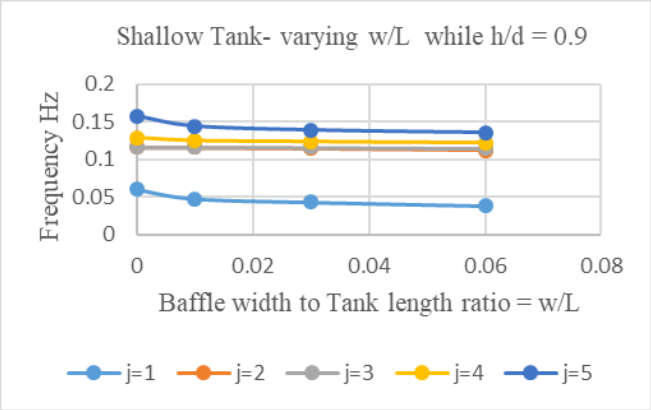


Fig. 6. Shallow Tank- Natural frequency variation of baffle width to tank length (w/L) while baffle height to fluid depth (h/d) =0.9

TABLE 7. FREQUENCIES (HZ) ON CENTRALLY PLACED BAFFLE WITH VARYING H/D AND W/L – TALL TANK

| d/L | h/d | j = mode number | w/L= 0 (No baffle) | w/L= 0.01 | w/L= 0.03 | w/L= 0.06 |
|---|---|---|---|---|---|---|
| 0.2 | 0.25 | 1 | 0.088 | 0.086 | 0.085 | 0.085 |
| | | 2 | 0.154 | 0.153 | 0.153 | 0.153 |
| | | 3 | 0.195 | 0.194 | 0.193 | 0.193 |
| | | 4 | 0.202 | 0.199 | 0.198 | 0.198 |
| | | 5 | 0.202 | 0.200 | 0.200 | 0.200 |
| | 0.5 | 1 | 0.088 | 0.062 | 0.080 | 0.078 |
| | | 2 | 0.154 | 0.086 | 0.153 | 0.153 |
| | | 3 | 0.195 | 0.162 | 0.193 | 0.192 |
| | | 4 | 0.202 | 0.195 | 0.195 | 0.194 |
| | | 5 | 0.202 | 0.198 | 0.200 | 0.200 |
| | 0.9 | 1 | 0.088 | 0.061 | 0.059 | 0.053 |
| | | 2 | 0.154 | 0.077 | 0.153 | 0.150 |
| | | 3 | 0.195 | 0.161 | 0.182 | 0.179 |
| | | 4 | 0.202 | 0.188 | 0.193 | 0.187 |
| | | 5 | 0.202 | 0.194 | 0.201 | 0.2 |

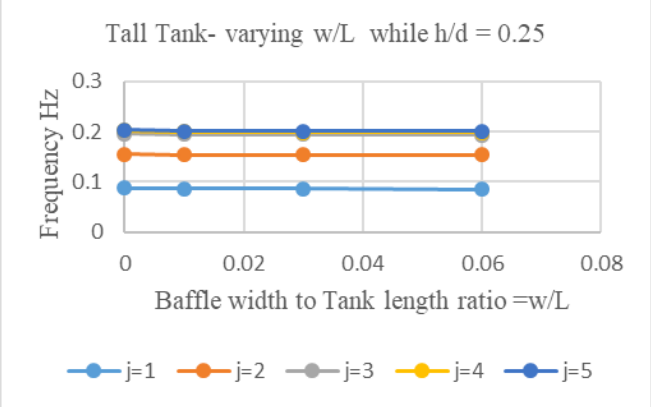


Fig. 7. Tall Tank- Natural frequency variation of baffle width to tank length (w/L) while baffle height to fluid depth (h/d) =0.25

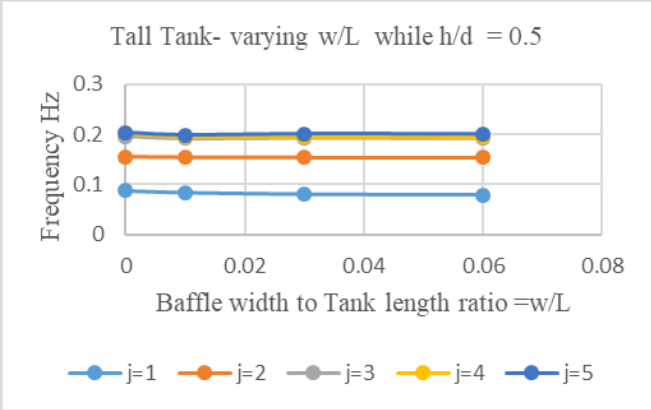


Fig. 8. Tall Tank- Natural frequency variation of baffle width to tank length (w/L) while baffle height to fluid depth (h/d) =0.5

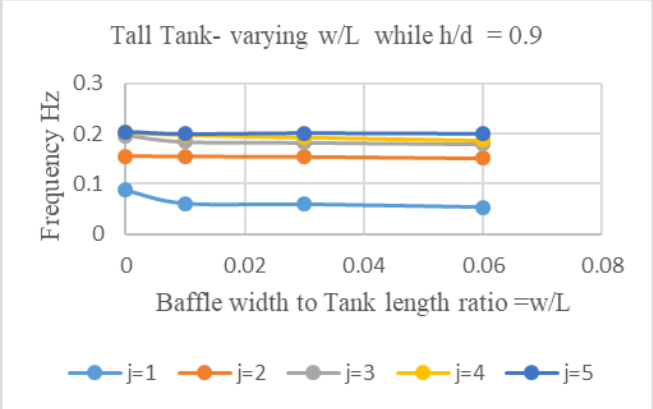


Fig. 9. Tall Tank- Natural frequency variation of baffle width to tank length (w/L) while baffle height to fluid depth (h/d) =0.9

In Fig. 4. – 9., a decrease in natural frequencies is observed with the increase of w/L of the centrally placed baffle of given height for both shallow and tall tanks. While the baffle height to fluid depth (h/d) is around 10-25%, the natural frequency deviation is not significant. However as the ratio of h/d increases beyond 90%, there is a notable impact of the baffle height in the decrease in frequency. Both the fundamental frequency and higher modes exhibit sensitivity to the baffle width.

### *2) The Effect of Baffle Height and Water Depth (h/d)*

To facilitate a comparison of the results, the parameters have been non-dimensionalized. Frequencies for both shallow and tall tanks are compared separately for selected w/L values while varying the h/d values.

For Shallow Tank:

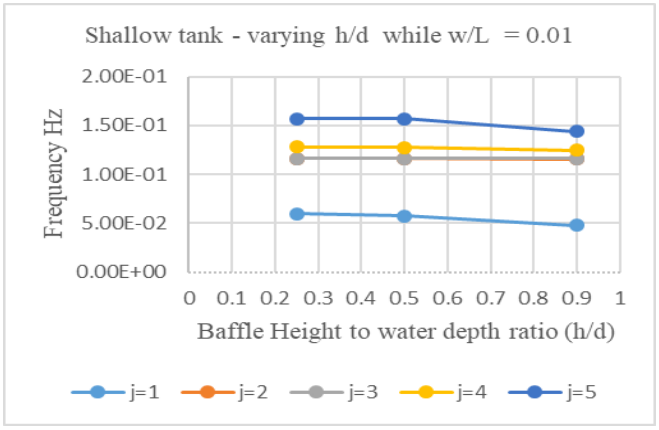


Fig. 10. Shallow Tank- Natural frequency variation of baffle height to tank depth (h/d) while baffle width to tank length (w/L) = 0.01

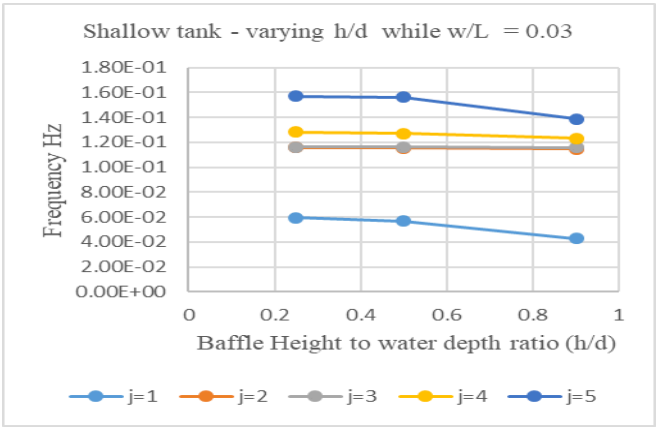


Fig. 11. Shallow Tank- Natural frequency variation of baffle height to tank depth (h/d) while baffle width to tank length (w/L) = 0.03

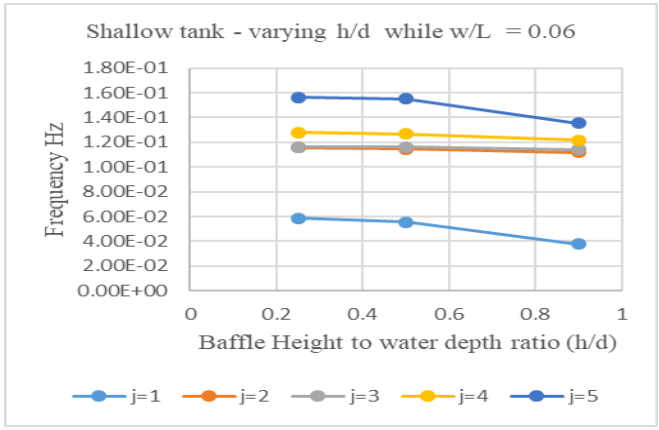


Fig. 12. Shallow Tank- Natural frequency variation of baffle height to tank depth (h/d) while baffle width to tank length (w/L) = 0.06

A decrease in natural frequencies is observed with the increase of centrally placed baffle height of a given width for both shallow and tall tanks. When, the baffle width increases three times and six times compared to the initial width, the natural frequency decreases for all the modes. It is unpredictable for which mode and for which baffle width, a significant deviation in the natural frequency occurs. The fundamental frequency is the most sensitive to baffle height.

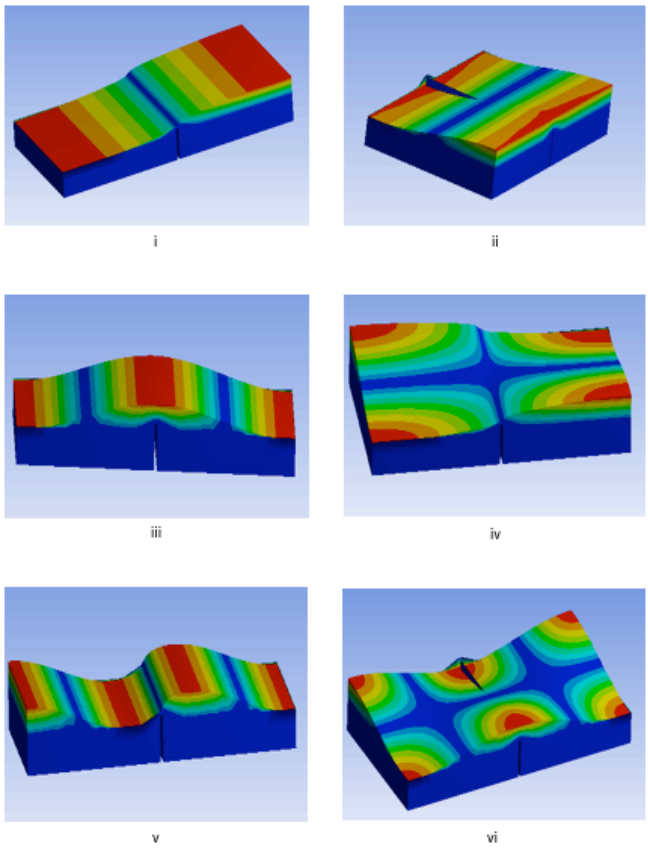


Fig. 13. Typical initial six mode shapes of single-centered shallow baffled tanks (only shown the mode shape of the liquid without tank in above figures)

### *3) The Effect of Baffle Location Along With Varying Baffle Heights*

Centered (0.5L) and off-centered (0.25L) baffle locations with varying baffle heights are considered for the natural frequency comparison for both shallow and tall tanks.

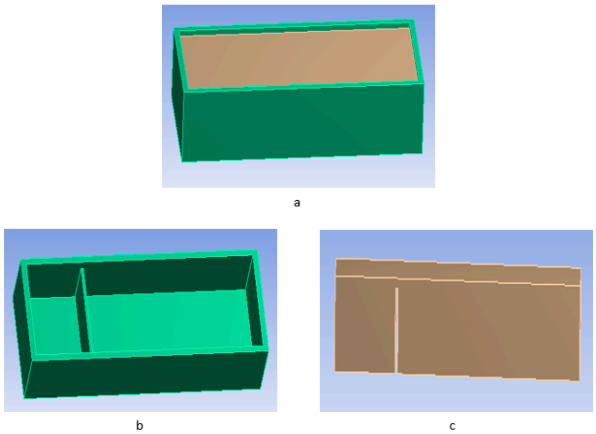


Fig. 14. a) 0.25L Baffled tank filled with fluid, b) 0.25L Baffled tank without fluid, c) Fluid without the tank

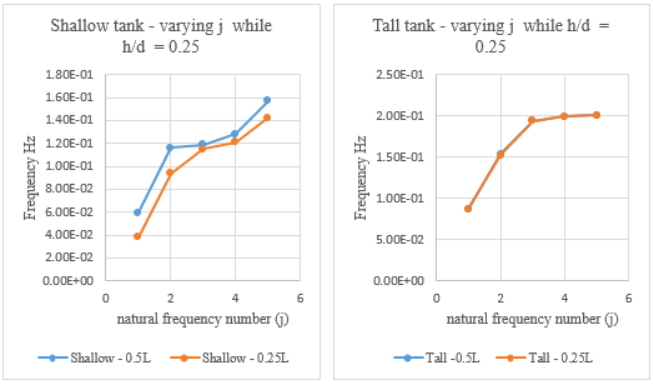


Fig. 15. Frequencies (Hz) on centred (0.5L) and off centred (0.25L) baffles with h/d = 0.25

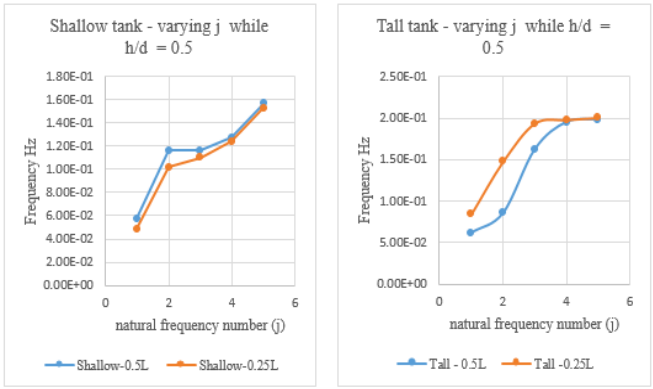


Fig. 16. Frequencies (Hz) on centred (0.5L) and off centred (0.25L) baffles with h/d = 0.5

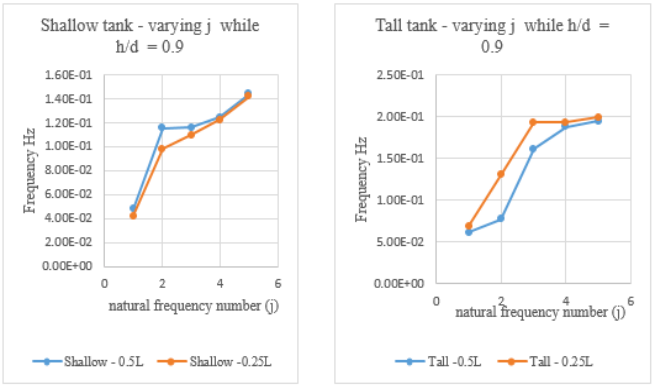


Fig. 17. Frequencies (Hz) on centred (0.5L) and off centred (0.25L) baffles with h/d = 0.9

When considering Fig. 15.–17., for the shallow tank when baffle height is increased, the mode frequencies are increased for both centered (0.5L) and off-centered (0.25L) baffle locations. In each mode (j value), centered (0.5L) baffle frequency is higher than the off-centered (0.25L) baffle frequency.

For the Tall tank when baffle height is increased, the mode frequencies are increased for both centered (0.5L) and off-centered (0.25L) baffle locations. In each mode (j value), off-centered (0.25L) baffle frequency is higher than the centered (0.5L) baffle frequency.

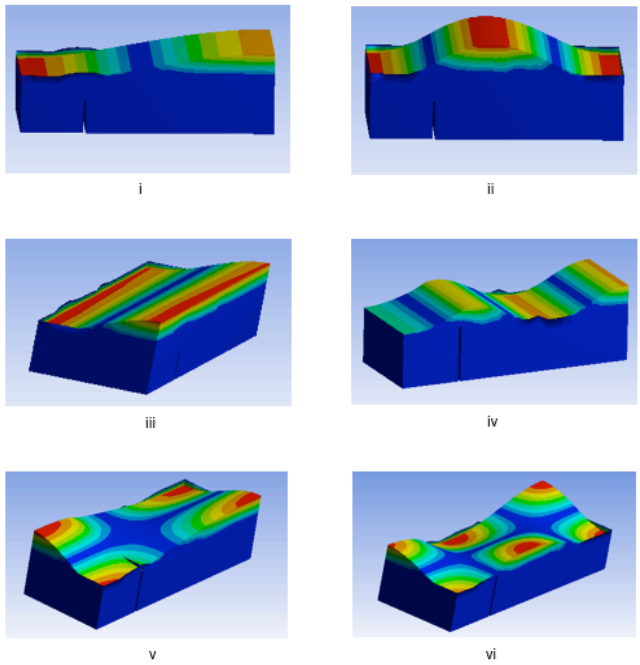


Fig. 18. Typical initial six mode shapes of single 0.25L Tall baffled tanks (only shown the mode shapes of the liquid without the tank)

*4) The Effect of the number of Baffles in Tanks for Frequency*

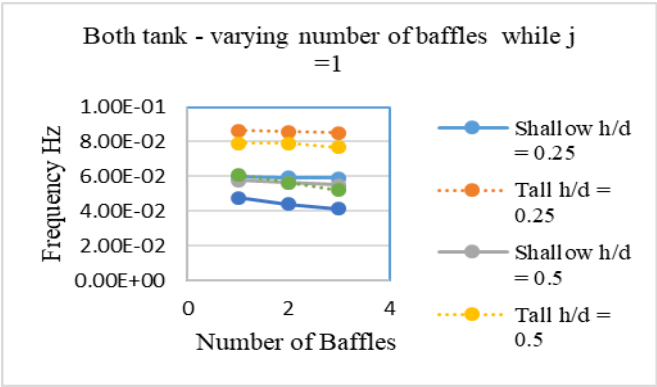


Fig. 19. Frequencies (Hz) on j =1 for varying h/d

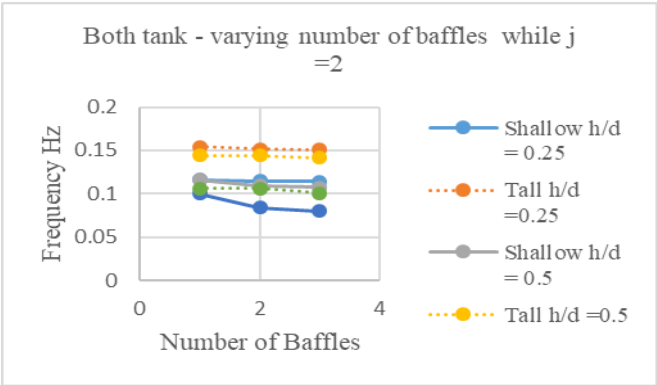


Fig. 20. Frequencies (Hz) on j =2 for varying h/d

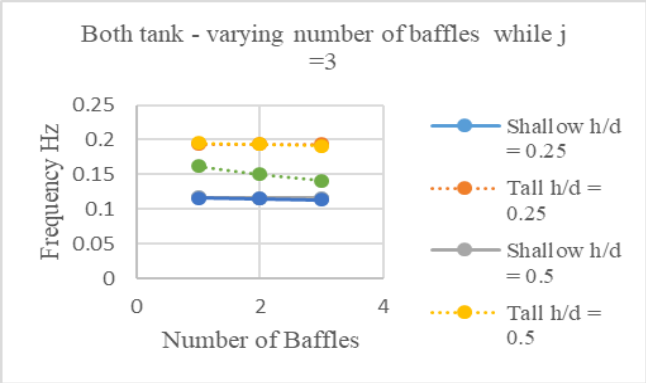


Fig. 21. Frequencies (Hz) on j =3 for varying h/d

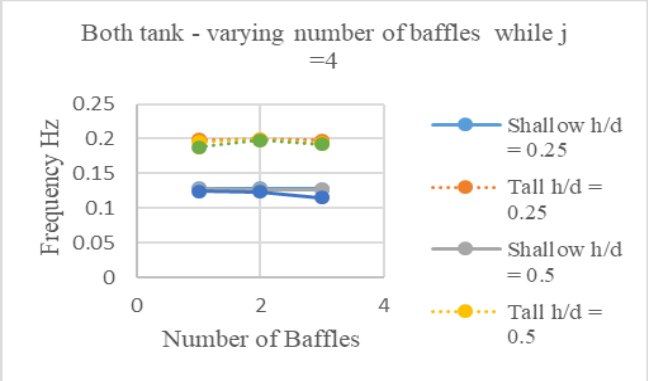


Fig. 22. Frequencies (Hz) on j =4 for varying h/d

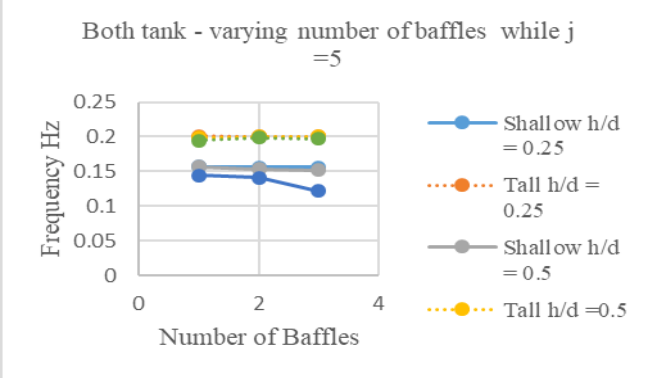


Fig. 23. Frequencies (Hz) on j =5 for varying h/d

In Fig. 19. – 23., the variation of baffle heights is considered. Considering the above figures, the general observation is when the number of baffles is increased, the frequency decreases for each frequency number (j). For the values j = 1,2, there is a significant decrease of frequencies when increasing the number of baffles for almost all the cases; i.e. for shallow and tall tanks h/d = 0.25,0.5 and 0.9.

## IV. Conclusions

1. The sloshing frequencies and the elevation of the free surface wave decrease as the height and width of the bottom-mounted submerged baffle increase. Among the baffle dimensions, the fundamental frequency is particularly sensitive to changes.

2. In the case of the shallow tank, when baffle height is increased, the mode frequencies are increased for both centered and off-centered baffle locations. In each mode, centered baffle frequency is higher than the off-centered baffle frequency. For the tall tank when baffle height is increased, the mode frequencies are increased for both centered and off-centered baffle locations. In each mode, off-centered baffle frequency is higher than the centered baffle frequency.

3. Taking into account the three parameters, the influence of the baffle height is prominent on both sloshing resonant frequencies and sloshing elevation.

4. The deviation of sloshing frequencies and mode shapes are mostly similar in the shallow tank and tall tank in similar cases due to the presence of the submerged baffle.

5. Generally, when the number of baffles is increased, the frequency decreases for each frequency number (j). For the values j = 1,2, there is a significant decrease in frequencies when increasing the number of baffles.

The fundamental frequency exerts more force than any other higher frequencies under external excitation. The stability of the considered tank is significantly impacted when the exciting frequency aligns with the fundamental frequency. In such instances, submerged baffles can be utilized to keep the fundamental resonant frequency or for that matter, any other resonant frequency away from the excitation frequency. In terms of constructional suitability, bottom-mounted vertical submerged baffles exhibit a more competitive influence over wall-mounted horizontal baffles. Submerged baffles prove to be more suitable than horizontal baffles in broad tanks, as changes in liquid depth may contravene the utility of horizontal baffles when the liquid level falls below the mounting height of the horizontal baffle. It can be concluded that the fundamental sloshing frequency of liquid in a tank can be kept away from the excitation frequency by adjusting the dimension, location, and number of submerged baffles.

## References

[1]. Ansys theory manual and Ansys explicit dynamics analysis guide2021

[2]. Ansys software 2019 R3

[3]. Housner, G. W., (1957), "Dynamic Pressure on Accelerated Fluid Containers", Bulletin of the Seismological Society of America, 47(1) 15-35.

[4]. Kianoush, M.R. and Chen, J.Z., (2006), "Effect of vertical acceleration on response of concrete rectangular liquid storage tanks" Engineering Structures, 28(5), 704–715

[5]. Chen, J.Z. and Kianoush M.R., (2005), "Seismic response of concrete rectangular tanks for liquid containing structures", Canadian Journal of Civil Engineering, 32, 739–752.

[6]. Kim, J. K., Koh, H. M. and Kwahk, I. J.,(1996), "Dynamic Response of Rectangular Flexible Fluid Containers", Journal of Engineering Mechanics, ASCE, 122(9), 807-817.

[7]. Yazdanian and Ghasemi, (2017), "Study on fundamental frequencies of cylindrical storage tanks obtained from codes and finite element method" Civil Engineering Infrastructures Journal, 50 (1): 135-149, a June 2017.

[8]. Safaa A.S, Mohamed S.G, Hany A.E.G. (2019)," Seismic Behavior of Ground Rested Rectangular RC Tank Considering Fluid-Structure-Soil Interaction" (IOSR-JMCE),vol.16,no.1,2019,pp.01-15